Evaluation of Tropical Cirrus Cloud Properties and Dynamical Processes Derived from ECMWF Model Output and Ground-Based Measurements Over Nauru Island

J. M. Comstock and J. H. Mather
Pacific Northwest National Laboratory
Richland, Washington

C. Jakob
Bureau of Meteorology Research Centre
Melbourne, Australia

Introduction

Identifying the mechanisms responsible for the formation of cirrus clouds is important in understanding the role of cirrus in the tropical atmosphere. Thin cirrus clouds near the tropical tropopause transition layer (TTL) can have significant impacts on the radiative heating in the upper troposphere. These clouds may also affect the transport of water vapor through the TTL into the stratosphere. The ability of large-scale models to correctly forecast tropical cirrus occurrence is important in predicting the role of these clouds on climate. In this study, we compare ground-based lidar and radar measurements of cirrus occurrence and optical properties over the Atmospheric Radiation Measurement (ARM) site located on Nauru Island with those generated by the European Centre for Medium Range Weather Forecasts (ECMWF) model.

We first compare cloud height and visible optical depth τ derived from measurements and model simulations over an 8-month period. Second, we discuss the different cirrus types observed in the tropics and the dynamic processes that are responsible for their formation. We then present a case study that illustrates the ability of the model to predict thin cirrus.

ECMWF Model Output and Cloud Parameterizations

For comparison with ground-based measurements, we use ECMWF model output, which has a 60-km horizontal resolution. A time series of hourly model variables are created using concatenated operational 12- to 35-hr forecasts for the grid point nearest Nauru. The cloud parameterization is a fully prognostic cloud scheme (Tiedtke 1993; Jakob 2001) and has a strong coupling between the convection and cloud scheme. Both cloud fraction and ice water content (IWC) have an explicitly modeled convective source.

Over the period of study, several changes were made to the ECMWF model. First, the vertical resolution changed from 50 levels to 60 levels on October 13, 1999, with extra levels added primarily to the boundary layer. The ice cloud parameterization was also changed in October 1999. The initial

cloud scheme had a single parameterization relating ice crystal fall velocity (V) to IWC. The new cloud scheme assumes the same V-IWC relationship for large particles (>100 μm), but for small particles (<100 μm) a zero fallspeed is assumed. These changes had a significant impact on cirrus characteristics and their subsequent radiative impact. For the time period between January 1998 and late 1999, the correlation of ECMWF and observed surface downwelling shortwave (SW) radiation at the ARM site located on Manus Island is rather poor (Figure 1), and the model generally overestimates high cloud amount. As of late 1999, the agreement becomes significantly improved. This transition coincides with changes made to the cloud parameterization that reduces the cirrus ice content in the upper troposphere.

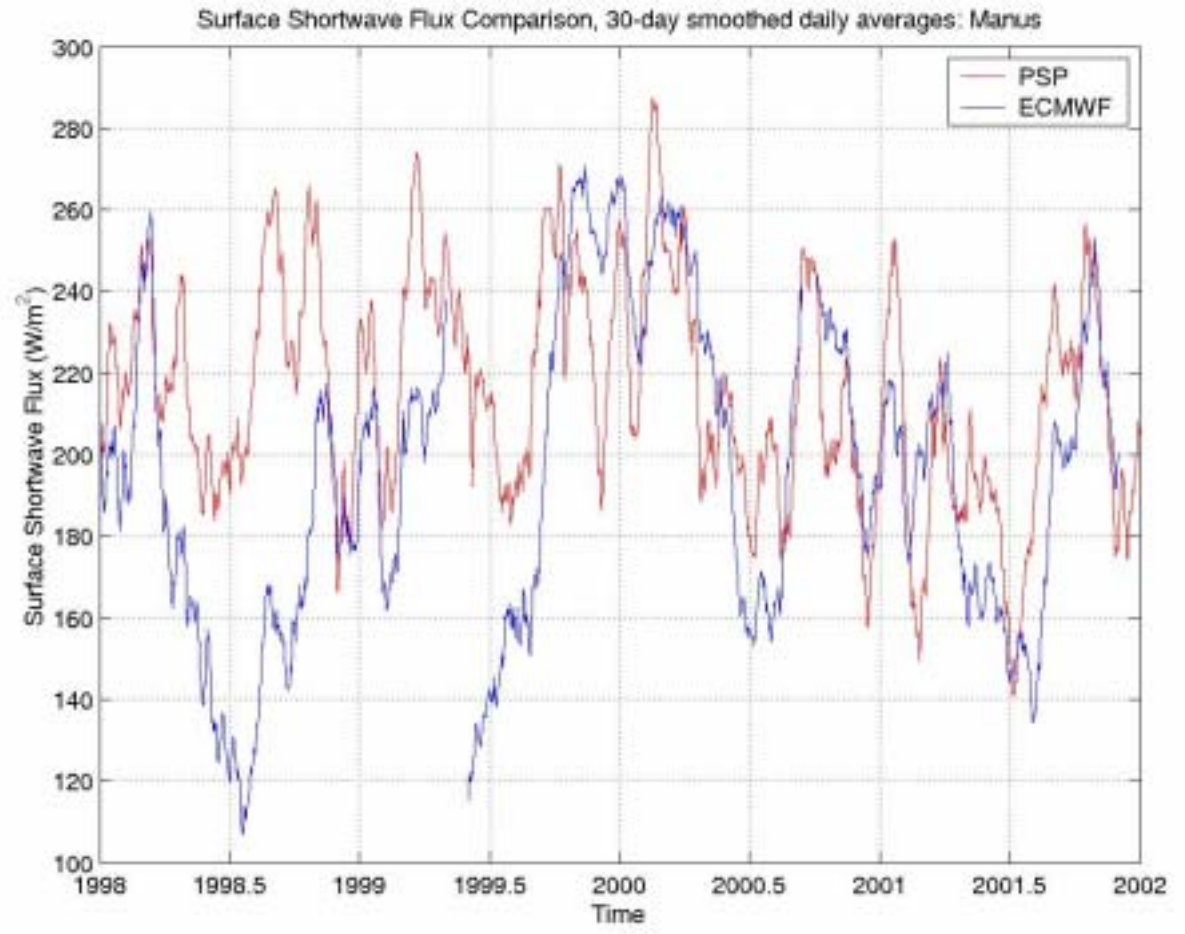

Figure 1. Comparison of surface SW flux measured at Manus and ECMWF model fluxes between January 1998 and December 2000.

Each grid box is subdivided into 100 sub-boxes to give 100 cloud configurations following an algorithm devised by Jakob and Klein (1999). The IWC (or liquid water content [LWC]) is assumed the same in each sub-box so that differences in τ arise from cloud cover variations with height and by applying cloud overlap rules to each sub-box. The model calculates τ using a relationship between ice water path (IWP) and temperature. Model cloud boundaries are identified by the presence of condensate (ice or water) in each atmospheric layer. Although there is some uncertainty when comparing model output for a 60-km grid box with single-point measurements, there has been some success comparing millimeter

cloud radar (MMCR) and ECMWF model cloud boundaries at the ARM Southern Great Plains (SGP) site (Mace et al. 1998).

Cloud Statistics

In this study, we use the Active Remotely-Sensed Cloud Locations (ARSCL; Clothiaux et al. 2000) algorithm to obtain cloud boundaries. This algorithm has the benefit of combining both micropulse lidar (MPL) and MMCR observations to obtain complete cloud boundaries. This is particularly important in the tropics where high cirrus clouds near the tropical tropopause are below the detection limit of the MMCR because they are optically thin and likely consist of small ice crystals (Comstock et al. 2002). For cloud conditions when low-level boundary layer clouds lie below cirrus layers, or optically thick anvil and middle level clouds, the MMCR provides better estimates of cirrus cloud top height because lidar is unable to penetrate through optically thick layers.

ARSCL cloud boundary statistics between April and November 1999 are compared with cloud boundaries output from the ECMWF model. Since most of the time period of this study lies before the cloud parameterization modifications mentioned above, we compensate for the model overestimation of high cirrus cloud amount by removing cloud occurrences when $\tau < 0.005$. This removes residual ice that exists in small quantities in the model upper troposphere.

Comparisons between model and measured cloud base and top frequency of occurrence for each month are in relatively good agreement (Figures 2 and 3), particularly in the months of May through August and October. Disagreement in September might be due to an overestimation of convective activity in the model that produced higher amounts of anvil cirrus over Nauru. Convective activity in the Nauru region was relatively suppressed during this month.

We use MPL measurements only to obtain cloud visible optical depth (Comstock and Sassen 2001). Lidar measurements are limited to clouds with $\tau < 3.0$. Previous studies have shown that radar and lidar retrievals of optical depths compare well for this time period at Nauru (Comstock et al. 2002). We compare visible optical depth derived using lidar observations with model output (Figure 4). As with cloud boundaries, the frequency of occurrence of τ is also in good agreement. There is a noticeable underestimation of $\tau < 0.1$ in the ECMWF model results for months April, July, and August.

Cirrus Cloud Dynamic Formation Mechanisms

Both model and observations show that tropical cirrus fall into two distinct categories: those observed near convection (anvils) and those observed detached from convection. Cirrus detached from convection are often thin, laminar in appearance, and located near the tropical tropopause. Anvil cirrus are usually physically and optically thicker than upper tropospheric (UT) cirrus located near the TTL and have more visible structure within the cloud. To assess the frequency that the ECMWF model predicts each cirrus type, we examine the convective rain present within a 1-hour window. Approximately 54% of cirrus forms when no precipitation is present in the grid box over the previous 1 hour.

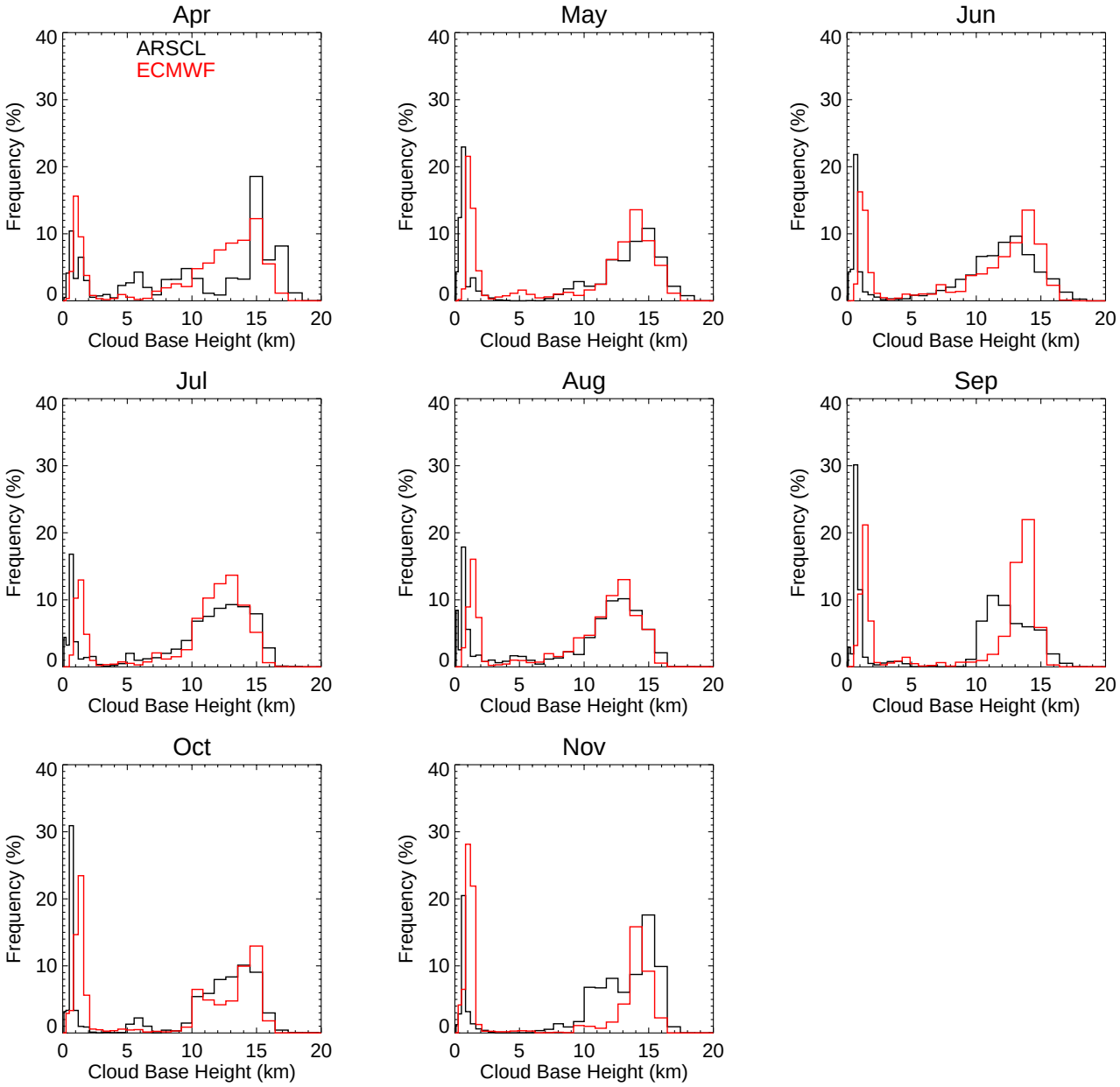

Figure 2. Monthly frequency of occurrence comparing ARSCL measured and ECMWF model cloud base heights between April and November 1999 at Nauru.

To determine how the model generates and maintains UT cirrus, we also extract the model large-scale vertical velocity associated with cirrus occurrence. Results indicate that 75% of all cirrus with cloud base $z_b > 7$ km and 77% of cirrus with $z_b > 15$ km occurs under conditions of large-scale ascent.

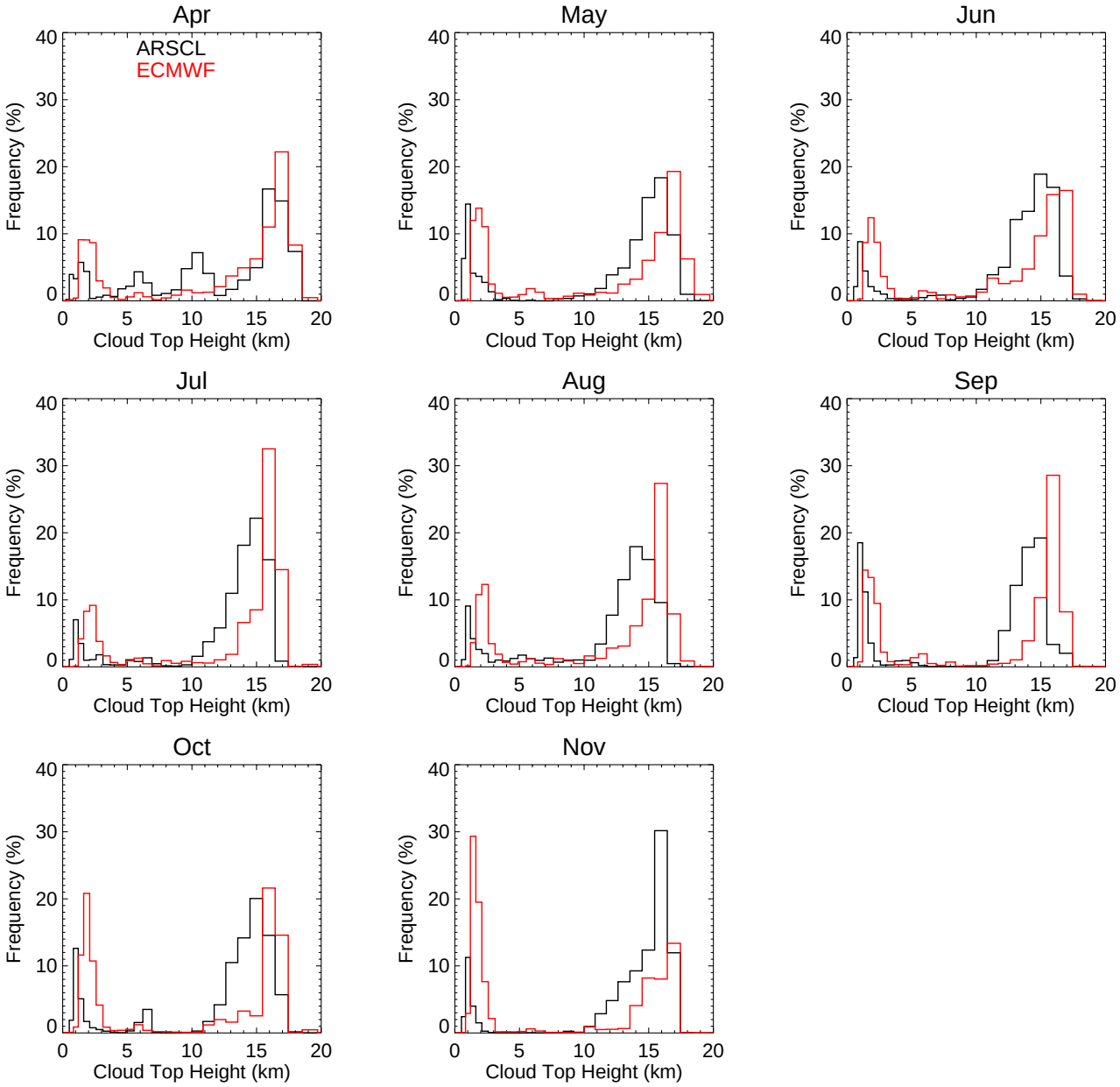

Figure 3. Monthly frequency of occurrence comparing ARSCL measured and ECMWF model cloud top heights between April and November 1999 at Nauru.

Analysis of a Thin Cirrus Case Study

To analyze the ability of the ECMWF model to predict specific cirrus cases observed over Nauru, we examined numerous cases that exhibited characteristics typical to anvil and UT cirrus clouds as judged by lidar and satellite measurements. Here, we compare measurements and model output for a thin cirrus case observed on September 21, 1999. For this typical UT cirrus case, a thin cirrus cloud was observed by the MPL at Nauru for nearly 12 hours (Figure 5b). The depth of this cirrus ranges from ~200 m to

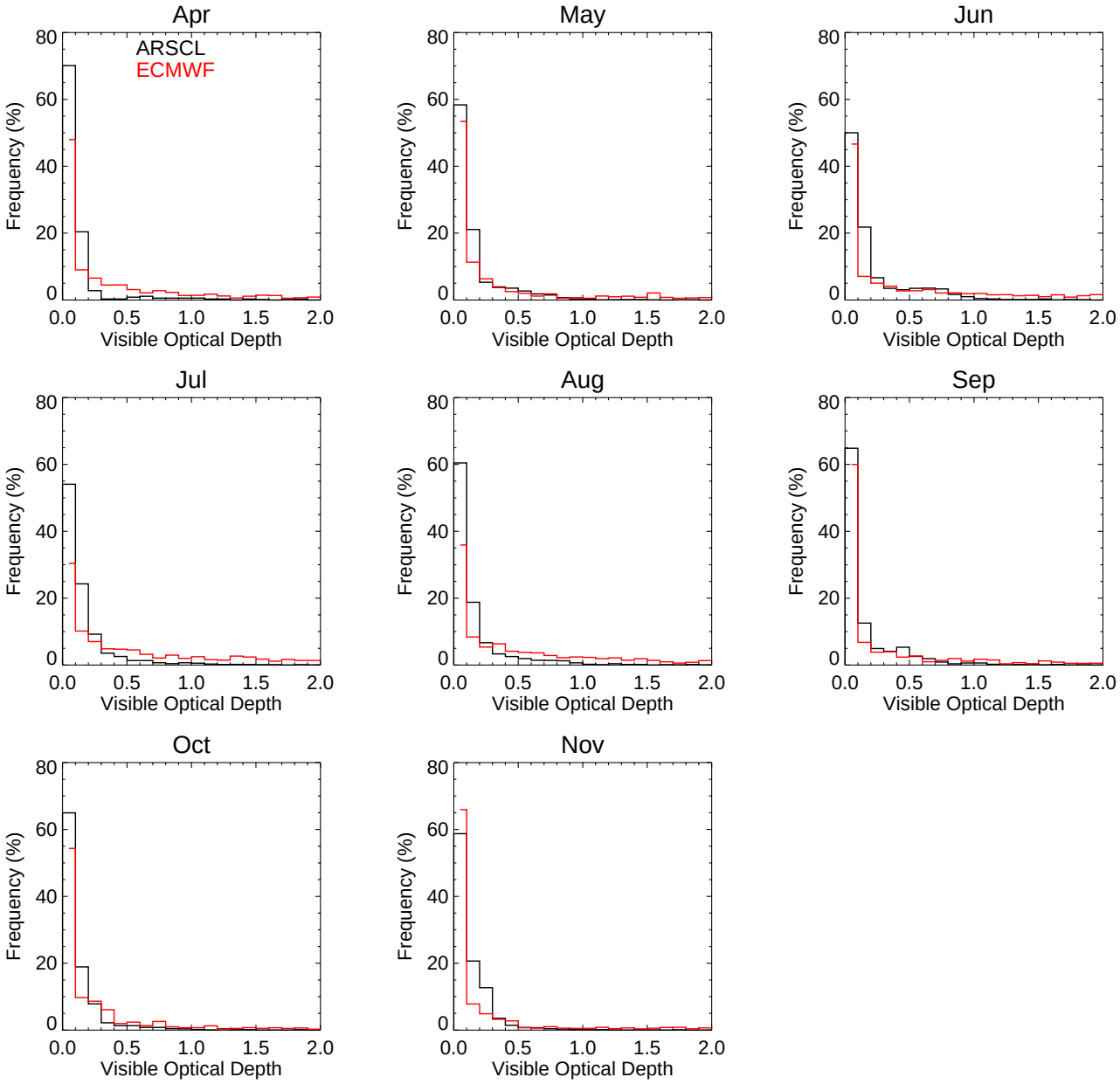

Figure 4. Monthly frequency of occurrence comparing lidar measured and ECMWF model visible optical depth between April and November 1999 at Nauru.

3 km and has an optical depth ranging from 0.001 to 0.05. Small-scale waves are apparent in the lidar backscatter image, particularly between 1300 and 1800 Universal Time Coordinates (UTC). Geostationary Meteorological Satellite (GMS) imagery indicates convection is not present in the region surrounding Nauru (Figure 5a). A 10-day back-trajectory analysis (Shoeberl and Sparling 1995) indicates that the air parcel associated with this cirrus event has undergone ~400 km of horizontal advection from the south. Examination of GMS imagery from 10 days prior reveals that the air parcel

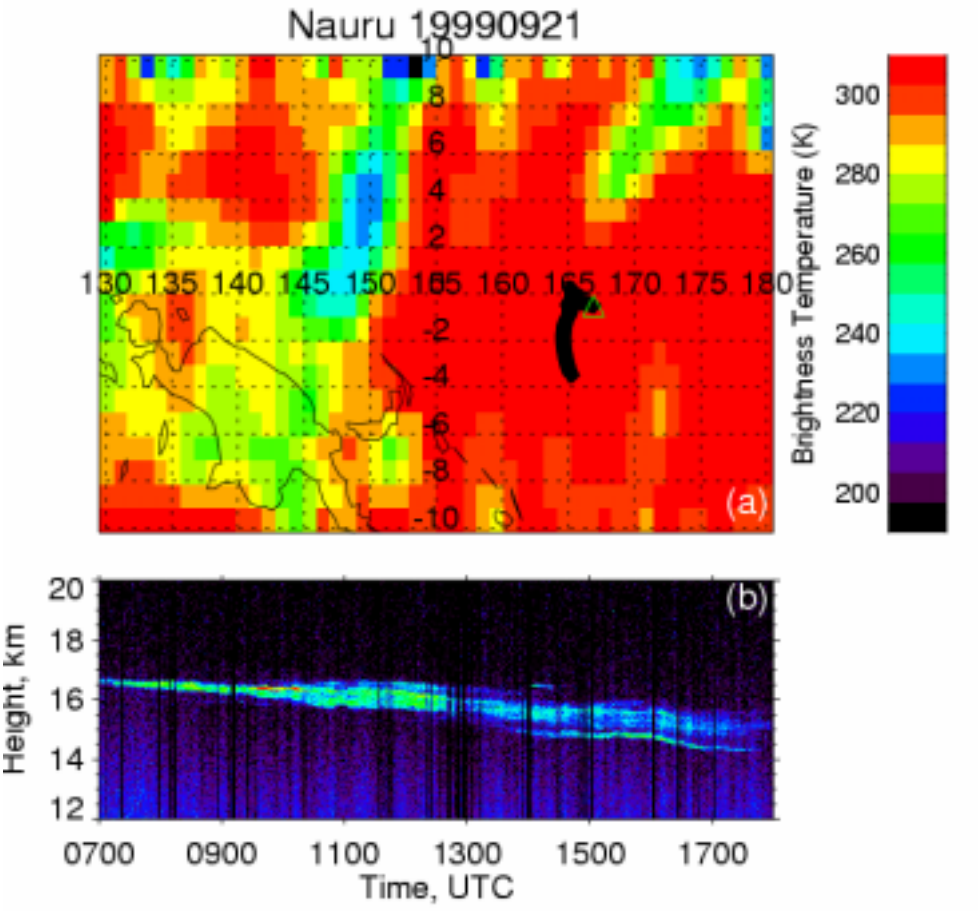

Figure 5. (a) GMS IR brightness temperature observed on September 21, 1999 over the Tropical Western Pacific (TWP). Nauru is located at 0.521 S 166.9 E (triangle) and the 10-day back trajectory is overlayed (black diamonds) on the satellite image. (b) Height vs. time display of normalized backscattered energy measured by the MPL at Nauru.

encountered convection to the south of Nauru 4 to 5 days before the thin cirrus observation. This implies that the source of the moisture for cirrus formation is likely convection, but the formation mechanism is likely another source (such as large-scale ascent or horizontal advection of moisture into a cold region).

On this day, the ECMWF model predicts thin cirrus above 15 km (Figure 6a) that occurs under conditions of large-scale ascent and high relative humidity (RH) (Figures 6c and d). The model predicts no precipitation in the grid box during the 24-hour period around the cirrus event. Also apparent in the model vertical velocity are tropospheric waves that appear to modulate the cirrus cloud cover and IWC. During periods of peak downward motion (red contours ~0800 UTC) the cirrus cloud cover and IWC decrease in magnitude. Thicker sections and higher IWC occur when the downward motion decreases (~0300 UTC). This correlation does not necessarily hold true at ~1400 UTC; however, the magnitude of the downward vertical velocity is not as strong. We found similar results after examination of several

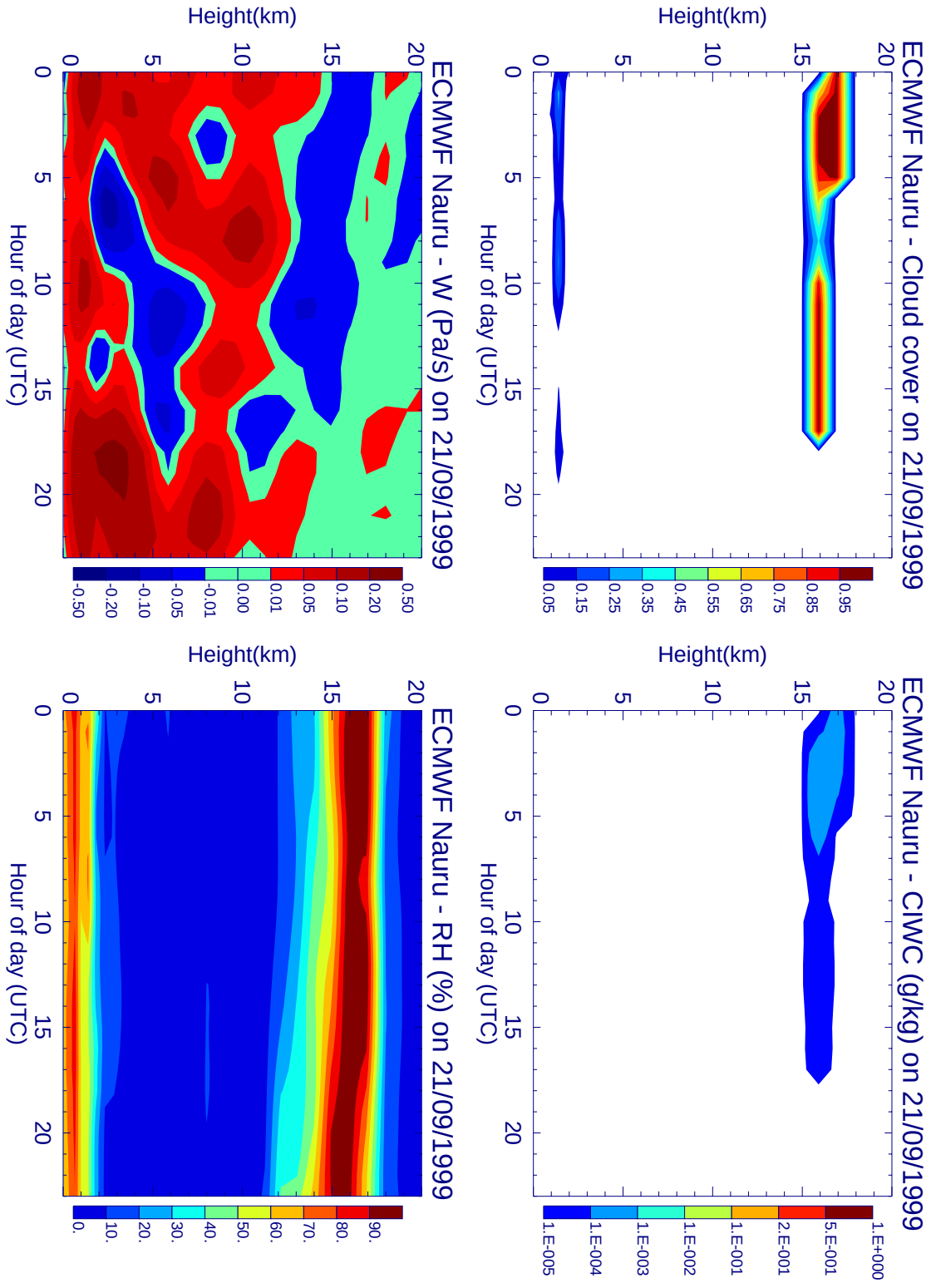

Figure 6. ECMWF model output for September 21, 1999. Results are averaged over 100 sub-boxes for the grid point nearest Nauru at each 1-hour time step. (a) Cloud cover, (b) IWC (g kg^{-1}), (c) vertical pressure velocity (Pa s^{-1}), and (d) RH (%).

UT cirrus cases. On occasion, the model failed to predict cirrus when it was detected by the lidar. This was due to insufficient water vapor and lack of vertical upwelling in the upper troposphere. These results show that the model predicts the formation of thin tropopause cirrus relatively well and tends to form under conditions of large-scale ascent. The source of the ascent is still uncertain at this point.

Summary and Future Work

In this study, we have compared cloud properties derived from the ECMWF model and measurements at ARM TWP sites. In addition to composite statistics, we also examined a thin tropopause cirrus case to evaluate the ECMWF model's ability to forecast UT cirrus and under what conditions. Although there is some difficulty comparing a model grid box with single-point measurements, our preliminary results show that the model predicts both convective anvils and isolated tropopause cirrus reasonably well. Cirrus persisting near the tropopause under convectively suppressed conditions occur when the model predicts overall ascent and high RH in the upper troposphere. Usually, RH is low and vertical velocity is generally downwelling in the lower troposphere during these time periods.

Although it seems obvious that tropopause cirrus forms when air is supersaturated and undergoes large-scale ascent, the mechanism that produces these conditions is not straightforward. A recent modeling study indicates that large-scale upwelling in the TTL may be the result of momentum transport by Rossby waves that are generated by tropical convection in the intertropical convergence zone region (Boehm and Lee 2003). Another study correlates cold temperature perturbations with tropical cirrus occurrence (Boehm and Verlinde 2000). Studying the frequency of these phenomena as well as identifying other mechanisms associated with the formation of tropical cirrus using the ECMWF model simulations and ARM Program measurements will be the subject of future work.

Corresponding Author

Jennifer Comstock, Jennifer.comstock@pnl.gov, (509) 372-4244

References

Boehm, M. T., and J. Verlinde, 2000: Stratospheric influence on upper tropospheric tropical cirrus. *Geophys. Res. Let.*, **27**, 3209-3212.

Boehm, M. T., and S. Lee, 2003: The implications of tropical Rossby waves for tropical tropopause cirrus formation and for the equatorial upwelling of the Brewer-Dobson circulation. *J. Amos. Sci.*, **60**, 247-261.

Clothiaux, E. E., T. P. Ackerman, G. G. Mace, K. P. Moran, R. T. Marchand, M. A. Miller, and B. E. Martner, 2000: Objective determination of cloud heights and radar reflectivities using a combination of active remote sensors at the ARM CART sites. *J. Appl. Meteor.*, **39**, 645-665.

Comstock, J. M., and K. Sassen, 2001: Retrieval of cirrus cloud radiative and backscattering properties using combined lidar and infrared radiometer (LIRAD) measurements. *J. Atmos. and Ocean. Tech*., **18**, 1658-1673.

Comstock, J. M., T. P. Ackerman, and G. G. Mace, 2002: Ground-based lidar and radar remote sensing of tropical cirrus clouds at Nauru Island: Cloud statistics and radiative impacts. *J. Geophys. Res*., **107**(23), 4714, doi:10.1029/2002JD002203.

Jakob, C., and Klein, S.A., 1999: The role of vertically varying cloud fraction in the parameterization of microphysical processes in the ECMWF model. *Quart. J. Roy. Meteor. Soc*., **125**, 941-965.

Jakob, C., 2001: The representation of cloud cover in atmospheric general circulation models. PhD-thesis, Ludwig-Maximilians-University, Munich, p. 193.

Mace, G. G., C. Jakob, and K. P. Moran, 1998: Validation of hydrometeor occurrence predicted by the ECMWF model using millimeter wave radar data. *Geophys. Res. Let*., **25**, 1645-1648.

Shoeberl, M., and L. C. Sparling, 1995: Trajectory modeling diagnostic tools in atmospheric science. *Proc. Int. School of Phys*., pp. 289-305.

Tiedtke, M., 1993: Representation of clouds in large-scale models. *Mon. Wea. Rev*., **121**, 3030-3061.